CFD Analysis Fireball Associated with an Aircraft Crash

Ashish V. Shelke[1*], Bhuvaneshwar Gera[2], Naresh K. Maheshwari[3], Ram K. Singh[4]
[1]PhD Scholar, Homi Bhabha National Institute, Mumbai, *ashishvshelke@gmail.com*
[2]Reactor Safety Division, Bhabha Atomic Research Centre, Mumbai, *bgera@barc.gov.in*
[3]Reactor Engineering Division, Bhabha Atomic Research Centre, Mumbai, *nmahesh@barc.gov.in*
[4]Department of Mechanical & Industrial Engineering, IIT Roorkee, *ramkumar.singh@gmail.com*

ABSTRACT: The accidental or intentional crash of aircraft causes the fuel spreading followed by a fireball formation. The experimental analysis of aircraft crash is difficult because of variation in each case. The fireballs in the case of aircraft crash are larger in size and radiates the larger amount of heat. The engulfment of such fireball may cause the local rise in temperature, which causes the spalling of concrete structure and fatalities to the human being. The semi-empirical model developed by the researchers gives the idea about maximum diameter, lifting height and surface energy emitted by the fireball. The transient behaviour of fireball and thermal hazards from it are analysed by using three-dimensional CFD code. The diameter and lifting height of fireball from video footage and OpenFOAM® analysis are matched well. The incident radiation and temperature achieved by the locations are also depicted. This method can use to study the effect of engulfing structure on the evolution of fireball and thermal hazard from the radiated heat to structure.

Keywords*: Aircraft Crash, Fireball, OpenFoam, CFD*

*****

1. INTRODUCTION

A fireball is defined as a ball of flame from sudden ignition and rapid combustion of concentrated flammable vapor [1]. The fireball is made from either single fuel or diluted mixtures. The fireball appears for relatively short duration and it passes through several distinct stages in its lifecycle [1]. Following are the different stages (1) growth of fireball (2) steady burning and (3) afterburning. In the growth of fireball, rapid mixing of released fuel and air occurs with rapid combustion due to available heat sources. The fireball is seems roughly spherical and changes to mushroom shape due to Rayleigh Taylor instability (friction with atmosphere air) in the stage of steady burning. The fireball size remains constant, but the flame becomes less sooty due to diffusion of combustion products in atmosphere and fireball becomes more translucent. The decisive parameters which helps to know about combustion of droplets or vapor cloud are described by researchers [2]–[7].

In the aircraft crash, it is often seen that the fuel in the aircraft tank (wings) is dispersed while crashing. Due to impact with crusing velocity, the failure of wing structure happens. Due to availability of heat source either from electronic short circuit or from jet turbine, the dispersed fuel will involved in combustion and results a fireball. The formed fireball radiates the large amount of heat and engulfs both combustible and non-combustible structures, which may causes the hazard to human. It is difficult to analyse thermal hazard associated with the aircraft crash by performing the experiments. There is need of Computational Fluid Dynamics (CFD) tools to deliberate the study of fuel dispersion, combustion and fireball formation. The evolution of fireball, heat radiated and thermal hazard during the lifetime of fireball are analysed in this paper using OpenFOAM-CFD code. The parameters of fireball are obtained using three-dimensional CFD simulations are compared with video footage data. This work can be useful where the thermal response of the structure and human being is important in case of aircraft crash.

2. AIRCRAFT AND FIREBALL

The past aircraft crashes provides the useful information regarding the fuel spreading, fireball or pool formation and hazardous effects of thermal radiation from the fire. We have divided the study of aircraft accidents in three major parts to understand the effect of structure with which aircrafts were crashed. Following subsections will explains crash cases with various impact conditions.

2.1 Impact with ground

The outcome of aircraft impact on the ground is either a fireball or a pool fire. The impact of aircraft with the ground surface is known as hard impact, because the aircraft structure is softer than that of ground. Some of the aircraft accidents with the ground with their causes and injuries are given in Table 1. The impact with hard structure is more eventually result into fireball and rare the case of pool fire. Pool fire is often observed in case where aircraft impacts with slower speed or with the soft terrains.

Table 1: Aircraft accidents with ground impact[8]

Aircraft Type	Date of incidence	Location	Cause and Injury
B772	5th September 2001	Denver, USA	Refuelling operative killed, when a fire broke out following the failure of a refuelling coupling
B742	24thJanuary 2005	Düsseldorf, Germany	The overrun led to collision with ground obstacles and two caught fire,
B762	2nd June 2006	Los Angeles, USA	Both engines and the aircraft sustained substantial damage from the fuel-fed fire
A310	10thJune 2008	Khartoum, Sudan	fuel-fed fire took place while stopping of aircraft with one inoperative thrust reverser
Bombardier DHC8-100	13thOctober 2011	Papua, New Guinea	A forced landing was made following which the aircraft caught fire, only one of the 29 passengers survived

2.2 Impact with structure of small height

A hijacked commercial airliner was intentionally crashed into the building in an act of terrorism [9]. One hundred eighty-nine persons were killed and a portion of the building was damaged by the associated impact, deflagration and fire. The impacting airplane was a Boeing 757-200 aircraft. According to the National Transportation Safety Board, the aircraft was traveling at 227 m/s on a magnetic bearing of 70 degrees when it struck the Pentagon. The aircraft had on board approximately 16500 kg of fuel at the time of impact. A Pentagon security camera located near the northwest corner of the building recorded the aircraft as it approached the building. The first photograph was captured an image of the aircraft when it was approximately 98 m (approximately at 0.42 second) from impact with the west wall of the Pentagon [9], [10]. The velocity of aircraft at the time of impact can be accurately estimated at 156 m/s. One of the wings was sheared off with spilling of aircraft fuel and fireball was generated. According to information provided by the National Transportation Safety Board, the aircraft had on board about 20,200 L of jet-A fuel at the time of impact. Based on images captured by the Pentagon security camera, it is estimated that about 2,200 kg of jet fuel was involved in the prompt fire and was consumed at the time of impact outside the building. This left about 13,800 kg as the estimated mass of the jet-A fuel that entered the building and contributed to the fire fuel load within the building. The fire damage to columns, beams, and slabs was limited to cracking and spalling in the vicinity of the aircraft debris [9], [10].

2.3 Impact with Tall structures

On11th September 2001, often referred as 9/11, hijacked commercial airplanes attacked twin towers of the World Trade Centre (WTC) in New York City. The towers were destroyed by a combination of the plane impacts and fire ignited by the fuel available in each plane. The hijacked plane hit the north tower was American Airlines, Flight 11, a 767-223ER. It was estimated by government sources that aircraft was carrying about 34,000 L of fuel and was flying at about 211 m/s [11]. The second hijacked plane was United Airlines, Flight 175, a Boeing 767-222, estimated by government sources to be carrying about 31,000 L of fuel and travelling at about 265 m/s. The aircraft fuel is ignited into large fireballs of 60 to 100 m diameter. The expansion velocity of the WTC fireballs from the video footages can be estimated to be ~20 m/s, which was also rooted by Baum and Rehm [12]. From the collapse analysis of both the WTC and the Pentagon it has been cleared that the fire phases and engulfment of fireball played active roles in the destruction of structures.

2.4 Experiments of aircraft crash

It is quite complex to study the actual aircraft crash with fuel spillage and ignition of fuel by various heat sources. Every aircraft crash is unique with respect to such parameters as fuel, air and runway temperature, aircraft crash velocity and local wind speed, fuel tank rupture geometry, fuel dump rates, and existence of potential ignition sources[13].

Tieszen has studied a Fuel dispersal modelling of aircraft impact scenario by using for C-141 transport accidents for the Defense Nuclear Agency's Fuel Fire Technology Base Program [14]. The model for the high-velocity regime was generated using a test series conducted at intermediate scale. The impact velocities in the tests conducted were in the range from 12 m/s to 91 m/s and angles of impact from 22.5° to 67.5°. Two fuel dispersal regimes were found based on impact angle and impact velocities. At intermediate normal impact velocity, fuel will leak from the damaged tank at a rate proportional to damage. At high normal impact velocity, complete structural failure of the wing fuel tanks occurs and fuel will splash on impact. Test results showed that

no liquid pooling occurred for impact velocities greater than 61 m/s, independent of the angle of impact. He found some pooling that occurred at lower velocities with liquid-layer of maximum thickness 5.25 mm.

NASA and the Federal Aviation Administration (FAA) conducted a joint program in 1984 for the acquisition [15], demonstration and validation of technology for the improvement of transport aircraft occupant crash survivability using a large Boeing 720, four engine and remotely piloted transport airplane in a controlled impact demonstration (CID). The CID impact was spectacular with a large fireball created by the third engine on the right side, enveloping and burning the aircraft.

Kuchta has presented in technical report that, in a survivable crash fire accident, the chance of human survival is greatly reduced when a massive fuel spillage occurs[4]. He illustrated an indication of the fuel dispersion hazard, where the fireball size was plotted against impact velocity for vertical fuel drops with 5 gallons of JP-4 and JP-8 liquid or emulsified fuels. He noted that the fireball hazard was tend to nearly comparable for the low and high flash point liquid fuels for the impact velocity is increased sufficiently (e.g. 60 mph). He also observed that the fireball associated with the ignition of a small fuel spillage engulfed a large area in flame. He stated the dependency of fireball diameter (ft) was one-half the impact velocity (mph) using 5-gal metal containers in fuel drops with the JP-4 jet fuel.

Fleeter et al. worked on aircraft fire safety with atomization and flammability of anti-misting kerosene [13]. Compared to the laboratory environment, significant scales are very large in a crash. Ruptures of several meters diameter with dump rates of hundreds of kilograms of fuel per second have occurred. Air speeds must be considered up to the maximum impact survivable crash speed, approximately 85 m s-1. Fleeter et al. compared and correlated of flammability results with those of the Lakehurst aircraft crash tests and the FAA large scale wing shear facility and conclude that all of the experiments (FCTA, mini wing, FAA wing shear) lie within the range of dominant turbulent shearing[13]. In that respect, they accurately model the aerodynamic breakup of an aircraft fuel spill. If any jet scaling effects do have importance they would tend to result in larger drops appearing in larger scale crashes. Since smaller drops form a more flammable mist, the laboratory experiments would be more critical than an actual crash in terms of flammable mist suppression.

The researchers like Miguel [16], Thomson and Caiafa [17], Moussa [18], Wolfson et al. [19], Piers [20], Large [21], Hayden et al. [22] and Mozingo et al. [23] studied the fireball associated with aircraft crash.

3. CASE CONSIDERED FOR THE STUDY

On 29th April 2013,the 747-400 aircraft of National Airlines N949CA, Afghanistan had departed on a cargo flight N8-102 from Bagram (Afghanistan) to Dubai, UAE with 7 crew and cargo consisting of 5 military vehicles [24]. The aircraft has crashed shortly after take-off from Bagram Air Base's runway 03 when the aircraft entered a stall. The aircraft impacted the ground at a high vertical speed, causing an explosion and fireball erupted into flames near the end of the runway within the perimeter of the Air Base. All seven crewmembers were killed in this accident. The plane had picked up the five vehicles at Camp Bastion, Afghanistan, and had taken on 53 tonnes of fuel at Bagram before taking off for Dubai. Parts of the aircraft that separated as result of the initial load was shifted. The following figures shows the images captured from video footage (Figures 1-4). In the initial duration two separate local flame areas are observed, which further merged to form a single fireball.

Figure 1: Impact of aircraft (B747) to the ground

Figure 2: Fuel spreading with fire

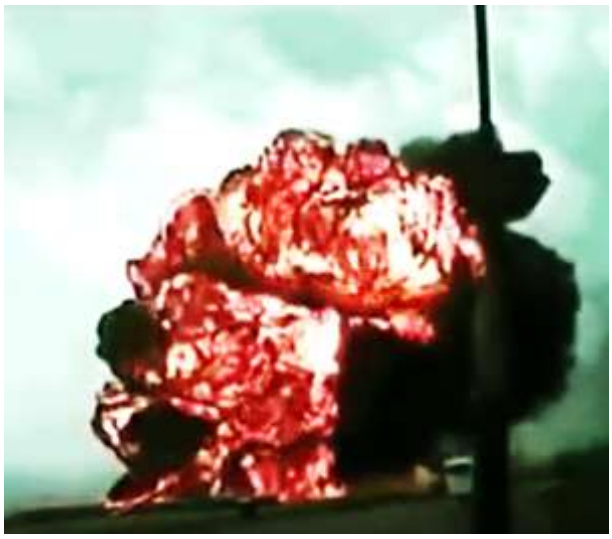

Figure 3: Formation of spherical fireball

Figure 4: Afterburning dispersion of fireball into atmosphere

.

Figure 5: Tow local areas of combustion observed in video footage.

4. SEMI-EMPIRICAL MODEL FOR FIREBALL

To estimate the percentage of the fuel contributing to the fireball, researchers have formulated many semi-empirical correlations. The developed correlations predict the maximum size, duration, lifting height, radiation and safe distance from hot fireballs. Following correlations for calculating fireball diameter and its duration are proposed by various authors based on their experiments,

$$D_{FB} = k_1 M_{fuel}^{n_1} \quad \text{and} \quad t_{FB} = k_2 M_{fuel}^{n_2} \tag{1}$$

where, M_{fuel} is the mass of fuel involved in fireball. The constants k_1, k_2, n_1 and n_2 used in the above correlations are given by [25]–[28]. The above mentioned empirical relations give idea about the maximum diameter and time duration of fireball. Martensen &Marx have given a dynamic model based on the experimental observations to track the time-varying behavior of fireballs [29].They suggested that the fireball tends to reach its maximum diameter during first third of fireball duration. The fireball starts lifting due to gain in buoyancy force therefore height of the fireball is also time dependent. Martensen & Marx [29] found the centre of fireball rises at a constant rate from the lift off position to three time the lift off position during the last two third of fireball duration. The Fireball can emit a large amount of radiant energy during its lifetime. This is capable of causing injuries and damage over an area several times greater than the size of the fireball [29]. A target close to fireball may be engulfed by it is of transient phenomena to know further distance at which engulfment occurs. In case where fireball is assumed expanding spherical and slightly settled on ground, the engulfment distance is approximated as its radius of during expansion.

These empirical models can only apply to recognize maximum diameter and duration of existence of fireballs. To understand the phenomena associated with combustion of fuel and flame structure inside the fireball, it is necessary to analyse fireball using CFD codes. There are assumptions made by researchers Fireball assumed to be isothermal and spherical in shape. In case where the fireball engulfs the structure the shape of fireball will not remain spherical. It is assumed by most of researchers that fireball radiates uniform heat but the radiative emission from a fireball varies over its surface. Moorhouse and Pritchard proposed upper limit of surface emissive power (SEP) of 300 kW/m^2 [30] while Roberts anticipated it as 450 kW/m^2 [31]. In case of larger fireballs the outer surface radiates heat faster and cools down its surface, the higher temperature remains inside the fireball due to combustion of fuel. So, the engulfment of fireball may cause the major loss inside the fireball in case of larger fireballs. To justify the assumptions by researchers there is a need of using CFD modelling for fireball from aircraft crash.

4.1 CFD Studies of aircraft

The numerical studies with fireball done by many researchers are deliberated for this paper (Makhviladze et al. [32], Makhviladze and Yakush [33], Luther and Müller [34], Rajendram et al. [35], Yakush and Makhviladze [36], Baum and Rehm [37], Shentsov et al.[38], Shelke et al.[39], Mishra et al. [40] and Wang et al. [41]. The CFD simulations of fireball from Boiling liquid evaporative vapour explosions (BLEVE) and aircraft crash are found identical in behaviour. Few authors have done simulations of fireball associated with aircraft crash.

Baum and Rehm [5] presented an analytical model based on an exact solution of the low Mach number of the initial expansion of a fireball. The solution was used to study the initial expansion of the fireballs generated in the attack on the World Trade Center (WTC) south tower. Video images were used to estimate the expansion rate of the fireball. From this information they estimated of the fuel consumed in the fireball by combining it with the analysis. They calculated the lifing velocity of fireball and validated with that obtained from video footage (~ 20m/s).

Luther and Müller [34] demonstrated FDS tool to simulate the effects fireball caused by the crash of a commercial airliner with Nuclear Power Plant (NPP) structures with 90 ton of kerosene. By using this tool, they measured potential hazard and developed the justifications. They studied the initial duration of the fireball before it rises above the NPP and the potential hazard of the flame front on the safety of the NPP. They presented impact of building structures on fireball evolution.

Shelke et al. [39] analyzed integral characteristics, which included diameter, lifetime, internal structure and flame structure inside the fireball using OpenFoam (fireFoam). The video footage data of aircraft accident were calculated using eddy dissipation combustion model (EDM) with single-step reaction coupled with the LES turbulence model. They calculated the incident radiation and maximum temperature achieved by the location to study of thermal hazards from the hydrocarbon fireballs.

5 CFD ANALYSIS

The simulations were carried out using FireFOAM module of OpenFOAM developed by Wang et al. It is an open source CFD software package[42]. The solver has advanced meshing capabilities including adaptive mesh and unstructured mesh and parallel computing capability. The FireFOAM module is embedded with turbulence model, combustion model, soot model, radiation model and pyrolysis model. The governing conservation equations and models used in FireFOAM are with Favre-filtered quantities [43].

$$\frac{\partial \bar{\rho}}{\partial t}+\frac{\partial}{\partial x_j}(\bar{\rho}\tilde{u}_j)=0 \tag{2}$$

$$\frac{\partial}{\partial t}(\bar{\rho}\tilde{u}_i)+\frac{\partial}{\partial x_j}(\bar{\rho}\tilde{u}_i\tilde{u}_j)=\frac{\partial}{x_j}\left(\bar{\rho}(\upsilon+\upsilon_t)\left(\frac{\partial \tilde{u}_i}{\partial x_j}+\frac{\partial \tilde{u}_j}{\partial x_i}+\frac{2}{3}\frac{\partial \tilde{u}_k}{\partial x_k}\delta_{ij}\right)\right)-\frac{\partial p}{\partial x_i}+\bar{\rho}g_i \tag{3}$$

$$\frac{\partial}{\partial t}(\bar{\rho}\tilde{Y}_k)+\frac{\partial}{\partial x_j}(\bar{\rho}\tilde{u}_j\tilde{Y}_k)=\frac{\partial}{x_j}\left(\bar{\rho}D_k\frac{\partial \tilde{Y}_k}{\partial x_j}-\overline{\rho Y_k''u_j''}\right)+\dot{\tilde{\omega}}_k$$

Where, $k=C_3H_8, C_{12}H_{26}, CO_2, H_2O$. (4)

$$\frac{\partial}{\partial t}(\bar{\rho}\tilde{h}_s)+\frac{\partial}{\partial x_j}(\bar{\rho}\tilde{h}_s\tilde{u}_j)=\frac{\partial}{x_j}\left(\Gamma_h\frac{\partial \tilde{h}_s}{\partial x_j}\right)+\frac{\partial p}{\partial t}+\overline{S_{rad}}+\overline{S_h}$$

$$\text{Where, } \Gamma_h=\left(\frac{\mu}{\mathrm{Pr}_h}+\frac{\mu_t}{\mathrm{Pr}_{th}}\right) \tag{5}$$

where ρ, u, p, h_s, Y denote density, velocity, pressure, sensible enthalpy and mass fraction of various gas species respectively. υ, υ_t, Pr_{th} denote laminar dynamic viscosity, turbulent dynamic viscosity and Prandtl number for enthalpy. D_k is the mass diffusion coefficient. ω_k is source term accounting for production or consumption of species "k". The superscript "-" donates the spatial filter and "~" donates the Favre filter. In the small Mach number approximation, it is assumed that, the pressure derivation of the ambient pressure is small and it can be neglected except the predictor and corrector step of the momentum equations. This approximation will eliminate the stiffness associated with the sound wave propagation. S_{rad} in the enthalpy equation is the source term accounting for thermal radiation. The turbulent viscosity is calculated based on One Equation Eddy model [44].

$$\frac{\partial \bar{\rho}k}{\partial t}+\nabla.(\bar{\rho}\tilde{u}k)=\nabla.(\bar{\rho}\nu_k\nabla k)+P-\varepsilon \tag{6}$$

where

$$P=-\bar{\rho}\cdot(D:B)$$

$$\varepsilon=c_\varepsilon\bar{\rho}^3\sqrt{k}\Delta^{-1}$$

$$B=\frac{2}{3}kI-2\upsilon_{SGS}.div(D)\ ,\ D=symm(grad(U))$$

Here, k and ε are the turbulent kinetic energy and dissipation rate of subgrid respectively, [45]. P is double inner product of two tensors D (Symmetric part of a rank 2 tensor created by the outer product of gradient and velocity vector and B (Sub grid stress tensor) and I is unity tensor [46]. The small Mach number approximation is used. This approximation excludes the stiffness associated with the propagation of sound waves. One Eddy Equation model used to calculate turbulent viscosity [46]. Infinitely fast chemistry assumed and combustion is analysed using Eddy Dissipation Concept (EDC) [47]. The EDC is modified version of eddy dissipation model, which is good approximation when the chemical kinetics is faster than overall fine structure mixing.

$$\dot{\tilde{\omega}}_k=-\frac{\bar{\rho}}{\tau_{mix}}\left(\frac{\chi}{1-\gamma^*\chi}\right)\min\left(\tilde{Y}_{fuel},\frac{\tilde{Y}_{ox}}{k}\right) \tag{7}$$

where, $\dot{\omega}_k$ is the reaction rate, τ_{mix} is turbulent mixing time, γ^* is mass fraction occupied by fine structure, χ is fraction of fine structure region which may react. Y_{fuel} and Y_{ox} are the mass fraction for fuel and oxidizer. The fuel used in calculation Kerosene ($C_{12}H_{26}$) (as physical and chemical properties of aircraft fuel found to be equivalent as that of Kerosene). Individual species transport equations are solved for the species O_2, H_2O, $C_{12}H_{26}$, CO_2 and N_2 to determine the gas composition. The following single step irreversible infinite reaction for kerosene as explained by Carlsson [48] is used.

$$2C_{12}H_{26} + 37(O_2 + 3.76N_2) \rightarrow 24CO_2 + 26H_2O + 139.12N_2 \quad (8)$$

The radiative heat transfer is solved using Finite volume discrete ordinates model (FVDOM)with weighted sum of grey gas model to evaluate the absorption, emission coefficient[49], [50]. The Soot model based on mixture fraction and scattering model are also incorporated. The equation of model is

$$\nabla.(I(\vec{r},\vec{s})\vec{s}) + (\alpha + \sigma_s)I(\vec{r},\vec{s}) = \alpha\eta^2 \frac{\sigma T^4}{\pi} + \frac{\sigma s}{4\pi}\int_0^{4\pi} I(\vec{r},\vec{s}')\phi(\vec{s},\vec{s}')d\Omega' \quad (9)$$

Where $\vec{r}$ $\vec{s}$ and $\vec{s}'$ are the radius vector, direction vector and scattering vector, respectively, *s, α, η* and σ_s denote the path length, absorption coefficient, refractive index and scattering coefficient. σ is the Stefan-Boltzmann constant. In addition *I*, ϕ and Ω' are the radiation intensity, scattering phase function and spatial angle respectively. CO_2 and H_2O are main contributors to flame radiation. The weighted sum of grey gas model is used to evaluate the absorption, emission coefficient [49], [50]. This model is regarded as a reasonable compromise between the oversimplified grey gas model and narrow band type models, which take into account particular absorption bands. Soot model and scattering are also incorporated with radiation model.

5.1 Initial and Boundary Conditions

The three-dimensional rectangular domain is selected to analyze both the fireball (Figure 6). The sizes of the domain has been selected based on preliminary calculations of maximum diameter and lifting height of fireball (from equation 1). The fuel inlet is in shape of wing and located at the centre of the bottom plane (XZ plane, y=0). The inlet face area taken as wing area and inlet velocity is calculated from the video footage. The inlet velocity is directed in Z direction for calculated time span. The time span of inlet is dependent on volume of fuel through inlet. As soon as the required fuel mass entered the computational domain, the inlet velocity was ramped down to zero. The acceleration due to gravity *(9.81m/s)* has taken in negative *Y* direction. The sides and top faces of the domain behave as open atmosphere, in which flow across the boundary of the domain is allowed. At *y=0*, the bottom plane of the domain behaves as ground where no-slip boundary condition is employed. The effect of air drag due to aircraft is also considered while applying the inlet boundary condition.

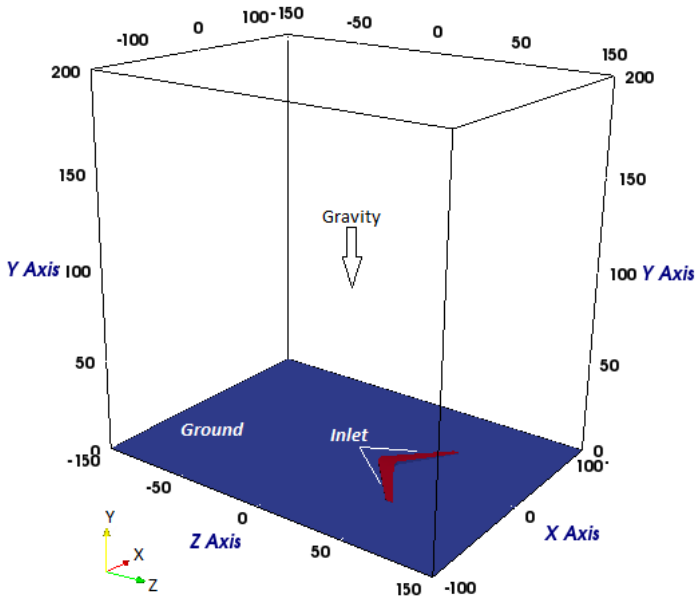

Figure 6: Schematic of computational domain showing the fuel inlet at y=0

5.2 Numerical Method

The discretized momentum, species transport and energy equations are solved by the preconditioned bi-conjugated gradient method (PBiCG). Generalized geometric-algebraic multi-grid method (GAMG) is employed to solve the discretized pressure equation originated from the application of momentum interpolation to the continuity equation. This method is also used to solve the discretized turbulent energy and the radiative transfer equations. The second order backward differentiation scheme is employed for temporal discretization. The diffusive terms and the gradients are discretized using central differencing scheme.

Spatial derivatives are estimated on a rectangular grid with all quantities assigned to the cell canter and velocities linearly interpolated to the cell faces. The FireFOAM employs the PIMPLE algorithm for pressure-velocity coupling. LES is solved in form of one equation with eddy coefficient of *0.07*. The energy equation is solved for sensible enthalpy. Temperature dependencies of the enthalpies and heat capacities of individual species have taken into account. The enthalpies of formation of various chemical species are available in JANAF thermochemical tables [51] and can be used in the most combustion simulation codes in the form of standard library.

6 RESULTS AND DISCUSSION

The present work is focused on the fireball formation only, the fuel spread in the form of chunks are not observed in video footage so they are neglected. It is assumed that total fuel mass in aircraft during accident got involved in fireball. The calculations are set up to run for 10.0 s and data are collected for every 0.01 s during the CFD simulation. In the study of fireball from two phase and single phase hydrocarbon by [52], it is found that evaporation is faster process than diffusion combustion and two phase release fireball behaves similar to single phase release. Hence, the fuel injected vertically from the wings located at ground (as shown in Figure 6), only gas phase fuel is considered. It is assumed that all the spilled fuel will vaporize and participate in fireball. For kerosene the latent heat of vaporization is small i.e. 246.85 kJ/kg as compared to heat of combustion i.e. 44.14 MJ/kg. Hence, evaporation phase is neglected. Results are discussed in following subsections.

Figure 7 shows the evolution of fireball at 2, 4, 6 and 8s. The fireball shows the similar behaviour as captured in video footages. The initial formation of two separate flame areas are also tracked during CFD simulation as observed in video footage (Figure 5). The initial local flame area is due to initial moment of fuel spreading and mixing of air-fuel. In the evolution it is also observed that the local area which is separated from the main fireball is burnt earlier due to limited availability of fuel and cooled faster. The fireball formation starts as kerosene fuel enters in to the domain. The fireball volume increases substantially since the fireball shape. It is seen that highest temperature was present inside the fireball due to process of combustion. Temperature of outer surface is lower and decreases rapidly due to heat radiation.

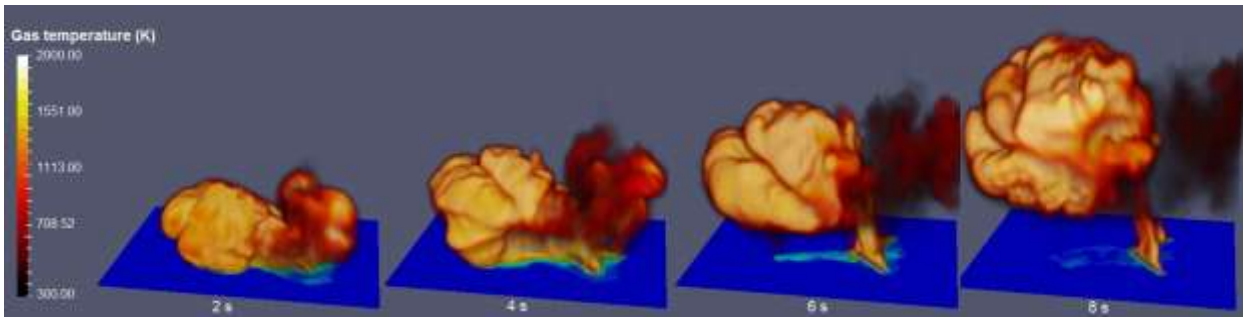

Figure 7: Fuel spreading with flame (2s), fireball formation (6s) and fireball lifting (8s)

Figure 8 shows the comparison of fireball diameter measured from the video footage and obtained in the simulation. The fuel spread in horizontal while aircraft crashed to ground. The fireball starts lifting due to buoyancy force as the density of product gases is low so the fireball is buoyancy dominated. The lifting of centre fireball from video footage and CFD simulation is compared in Figure 9. The accuracy associated with the process of fireball parameter measurement such as diameter and lifting height is high, because the portion of fireball and the surrounding phase are distinctly observable. It can be seen that a good agreement is found with that obtained from video footage of the accident. The lifting height calculated from OpenFOAM® analysis also matches with calculated height in video footage.

 ISSN: 2321-8169
152 – 167

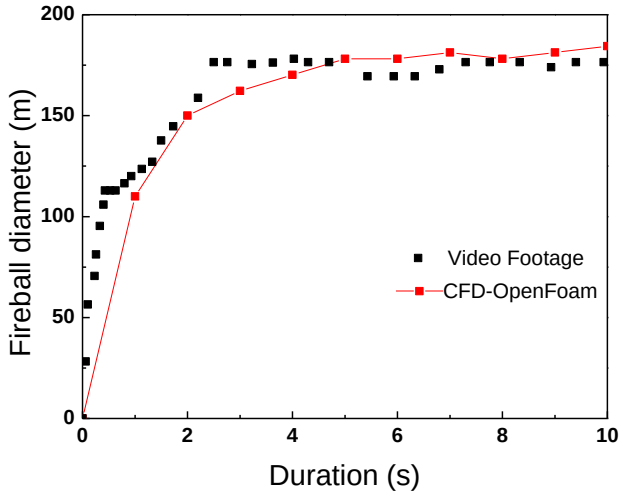

Figure 8: Comparison of fireball diameter from video footage and CFD simulations

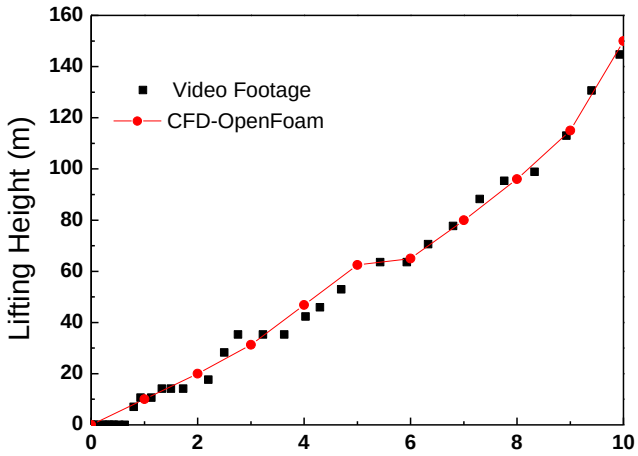

Figure 9: Comparison of lifting height of fireball using video footage and CFD simulation

To analyse the evaluation of fireball and thermal hazard analysis are deliberated by measuring the various parameters at located probes. The probes are located at 0,10,20,30 and 40 m in the Z direction away from the wings of aircraft (here, inlet of fuel in the domain) along the axis of aircraft (passing through nose and tail). The location of measuring probes are shown in Figure 10.

 ISSN: 2321-8169
152 – 167

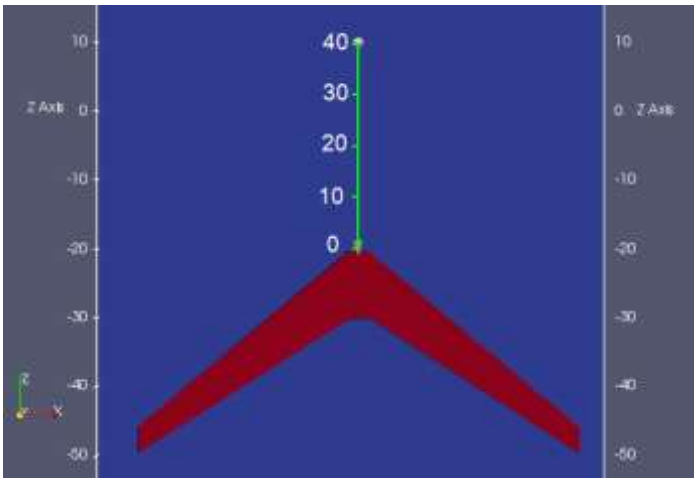

Figure 10: The location of probes for calculation of various properties

Figure 11 andFigure 12 show the mass fraction of fuel and CO_2 with time at different locations respectively. It is observed that fireball burnt mainly at outer surface due to availability of oxygen from surrounding air. Figure 11 shows the rapid decrease in fuel mass fraction at the locations 10 and 20 m away, while at the 0 m it remains higher for longer duration. In the Figure 12, the CO_2 mass fraction shows the higher value for longer duration. The stem of fireball existed at this location. While fireball starts lifting due to buoyancy, it drags the surrounding fresh air from the bottom side. The fresh air entered inside the fireball mixes with the remaining fuel and continues the combustion process.

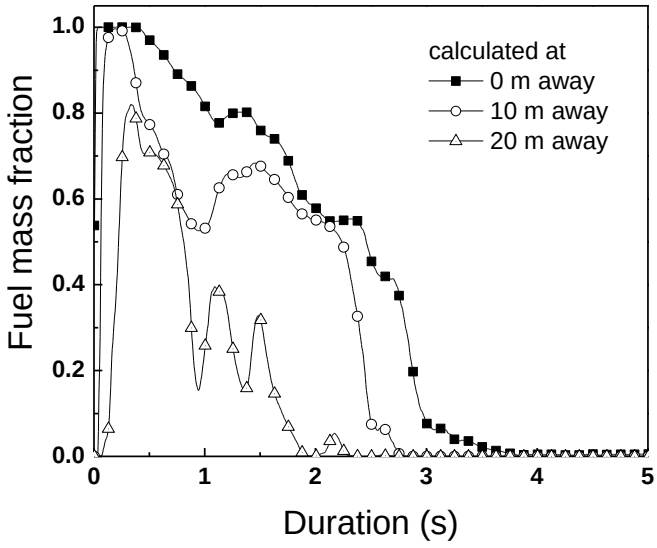

Figure 11: Fuel mass fraction plotted along Z axis (0, 10 and 20 m away)

 ISSN: 2321-8169
152 – 167

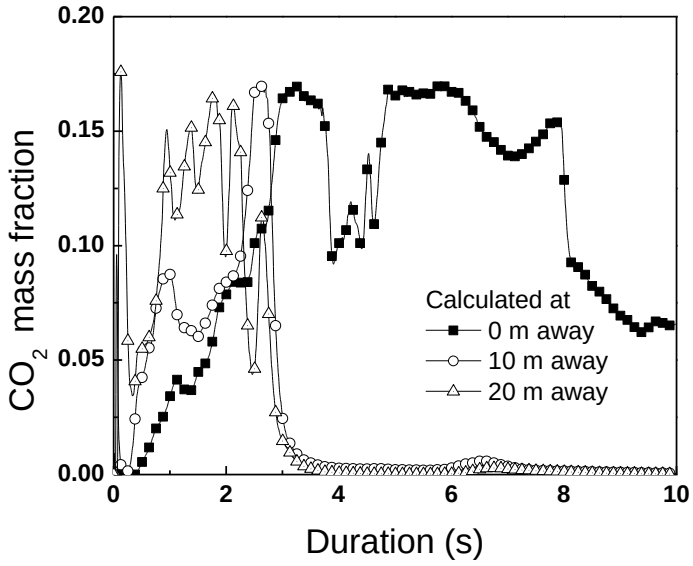

Figure 12 CO_2 mass fraction calculated in Z direction (0, 10 and 20 m away)

Figure 13 shows the amount of heat released during the lifetime of fireball. It is emphasized that, maximum amount of heat release rate (HRR) occurs very instantly within 0.2 s. The HRR reaches to a peak value of 1.1× 106 MW at around 0.05 s. The HRR remains constant around 0.3× 106 MW up to 8 s and then reduces sharply due to heat losses through open boundaries. This concluded that, the larger amount of fuel was burning until the time of 8 s.

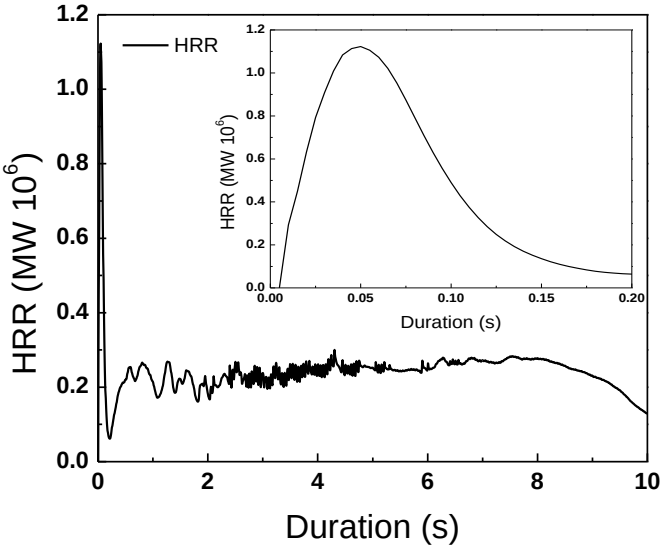

Figure 13: Heat Released Rate (HRR)

Figure 14 shows the time varying temperature profiles on ground surface (XZ plane, at y=0). It can be observed that there is a drop in the temperature towards the outer boundary due to radiating heat transfer to the atmosphere. The temperature of ground engulfed by fireball is close to flame temperature, as the inner zone of fireball does not lose heat through radiation/convection. From the temperature contour analysis it is found that the fireball starts lifting at 3 s and then the area engulfed by fireball on the ground reduces rapidly. This can be observed in Figure 15.

 ISSN: 2321-8169
152 – 167

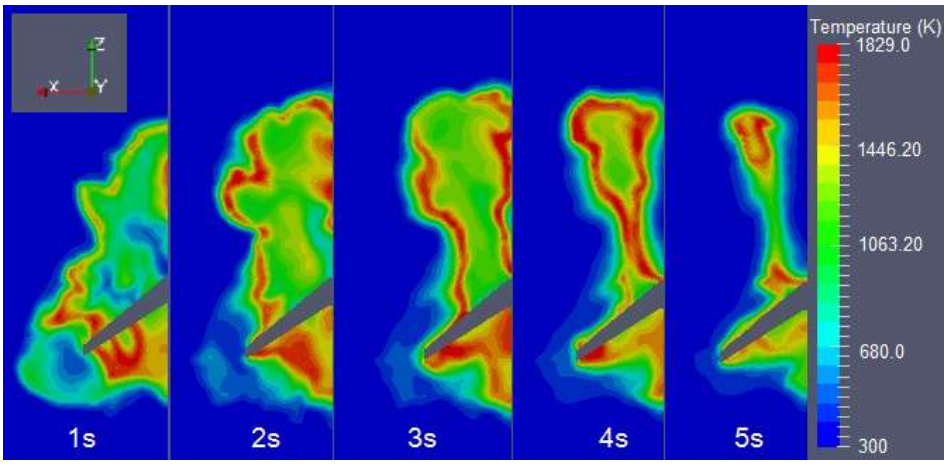

Figure 14: Temperature contours calculated on ground

Figure 15 shows the temperature probed at the locations of 0, 10 and 20 m. The rapid decrease in the temperature at 10 and 20m express the lifting of fireball. The temperature at 0 m shows the higher value for longer duration and gives the idea about most hazardous zone in thermal priority. The temperature profile for 30, 40 and 50 m away are depicted in Figure 16. The temperature profile shows the higher temperature for shorter duration. The outer surface of fireball cools rapidly and radiates lower amount of heat. The probes away from the fireball are less affected by the heat inside the fireball as the fireball in optically thick. These distance also helps to illuminate the the idea of safest distance to observe the fireball. Due to limitation of computational domain author is unable to find safest distance.

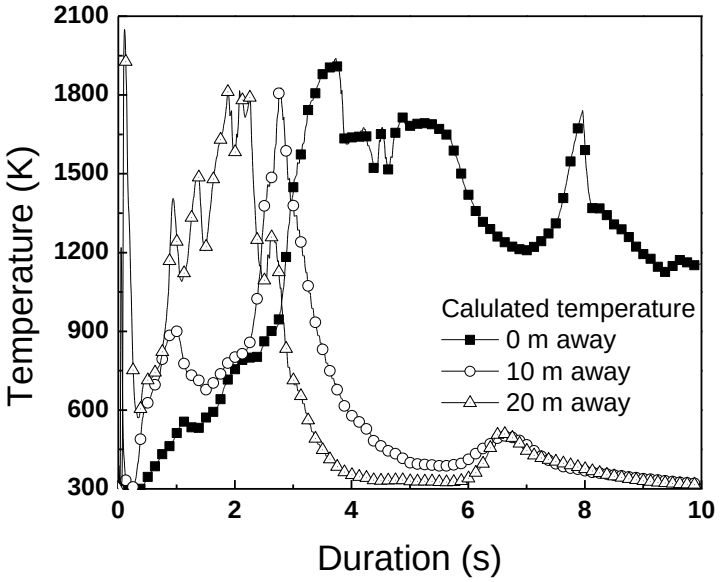

Figure 15: Temperature calculated in Z direction (0, 10 and 20 m away)

 ISSN: 2321-8169
152 – 167

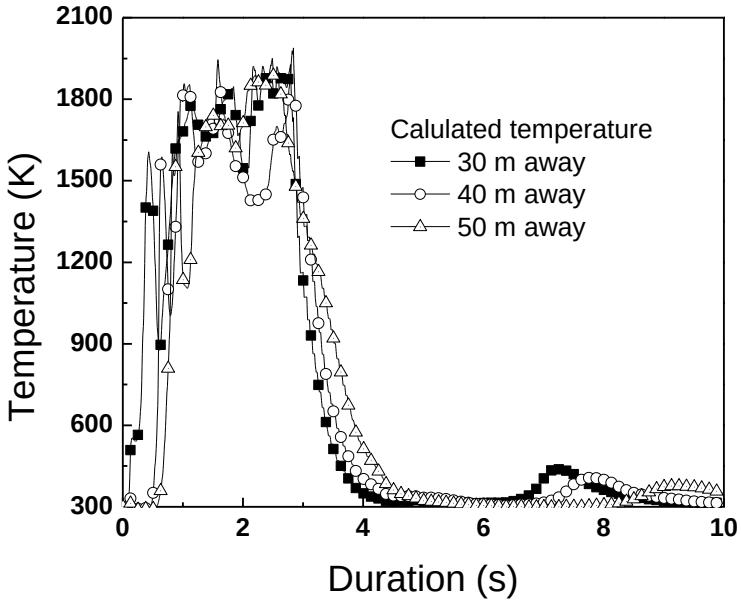

Figure 16: Temperature calculated in Z direction (30, 40 and 50 m away)

Figure 17 demonstrates the pressure measured by the probe locations during simulations. The pressure is generated due to expansion of product gases. The maximum pressure of 2×10^5 N/m^2 is observed at the probe location of 10 m at 0.05 s. The process of combustion studied in this paper is purely deflagration in nature as the pressure generated is low in magnitude and shorter in duration.

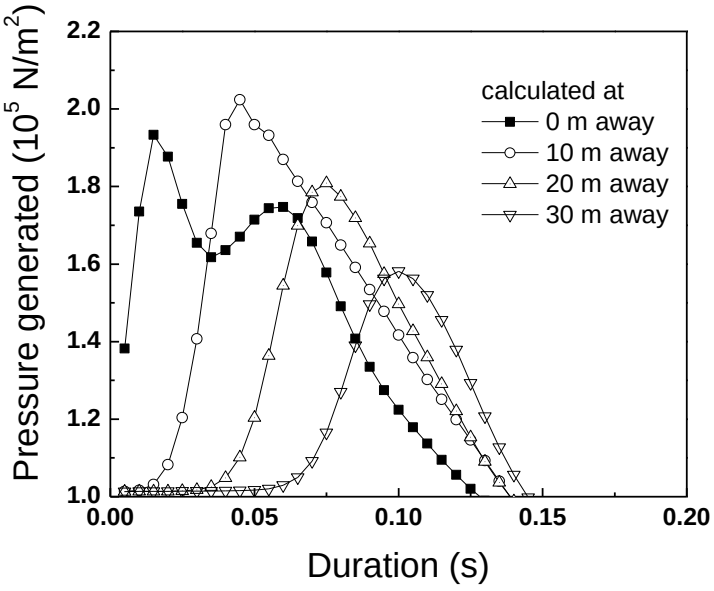

Figure 17: Pressure Calculated in Z direction (0, 10, 20 and 30m)

Figure 18 shows the velocity traced at the probe locations of 0, 10, 20 and 30 m away. The velocity observed at 0, 10 and 20m locations of nearly 200 m/s for the 0.2 sec duration. The increase in velocity (100 m/s at inlet) is due sudden combustion and expansion of product gases. The probe at 30 m shows the velocity peak of 150 m at 0.5 s. The reduction in the velocity is due to

atmospheric friction while expanding of gases. After 1.5 s the velocity at the probe locations quickly decreases. This emphasized the decrease in effect of initial moment in the direction of probes.

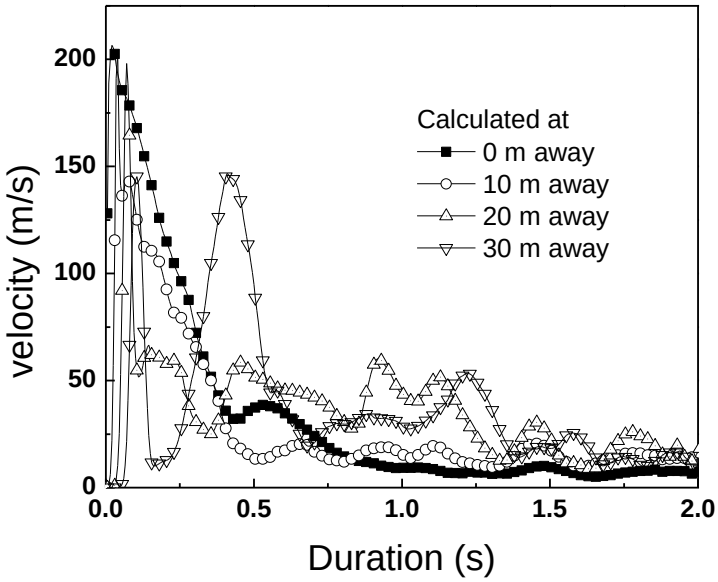

Figure 18: Calculated velocity in Z direction (0, 10, 20 and 30m)

7 CONCLUSION

CFD analysis has been carried for fireballs using FireFOAM. The overall agreement between the simulated ad observed data encourages the use of FireFOAM in thermal analysis of aircraft accidents. The fireball diameter and lifting height obtained in the CFD simulations are comparable to observed data. The spatial distributions of fuel and product mass fractions as well as the temperature helped to understand initial effect of momentum of fireball on its evolution. The effect of structures on the evolution of fireball and the thermal hazard on the surface of structure can be the areas of future scope this article. Following major conclusions are drawn from this article,

- The inner zone of fireball does not lose heat through radiation/convection; hence the temperature of inner zone of fireball is close to adiabatic flame temperature in both the cases. The fireball temperature is 2000 K
- The temperature predicted at area engulfed by fireball is of 1829 K near the flame temperature, which is high enough for spalling of concrete structures as well as human fatalities.

REFERENCES

[1] F. Lees, *Lees' Loss prevention in the process industries: Hazard identification, assessment and control*. Butterworth-Heinemann, 2012.
[2] J. A. Abbott, *Prevention of Fires and Explosions in Dryers: A User Guide*, no. 432. IChemE, 1990.
[3] A. M. Cruz, L. J. Steinberg, and R. Luna, "Identifying hurricane-induced hazardous material release scenarios in a petroleum refinery," *Nat. Hazards Rev.*, vol. 2, no. 4, pp. 203–210, 2001.
[4] J. M. Kuchta, "Fire and explosion manual for aircraft accident investigators," 1973.
[5] R. Rehm *et al.*, "Initial Model For Fires In The World Trade Center Towers," *Fire Saf. Sci.*, vol. 7, pp. 25–40, 2003.
[6] W. M. Pitts, "Wind effects on fires," *Prog. Energy Combust. Sci.*, vol. 17, no. 2, pp. 83–134, 1991.
[7] P. A. Croce and K. S. Mudan, "Calculating impacts for large open hydrocarbon fires," *Fire Saf. J.*, vol. 11, no. 1–2, pp. 99–112, 1986.
[8] "Skybrary." [Online]. Available: http://www.skybrary.aero/index.php. [Accessed: 05-May-2017].
[9] P. F. Mlakar, D. O. Dusenberry, J. R. Harris, G. Haynes, L. T. Phan, and M. A. Sozen, "The Pentagon building performance report," 2003.
[10] J. P. Spinti, J. N. Thornock, E. G. Eddings, P. J. Smith, and A. F. Sarofim, "Heat transfer to objects in pool fires."

[11] FEMA, *world trade center building performance study, executive summeary*. 2001, pp. 1–7.
[12] H. R. Baum and R. G. Rehm, "A simple model of the World Trade Center fireball dynamics," vol. 30, pp. 2247–2254, 2005.
[13] R. Fleeter, R. A. Petersen, R. D. Toaz, A. Jakub, V. Sarohia, and N. Aeronautics, "Antim isting Kerosene Atomization and Flammability," 1982.
[14] S. R. Tieszen, "Fuel Dispersal Modeling for Aircraft-Runway Impact Scenarios," *sandia Rep.*, no. November, 1995.
[15] K. E. Jackson, R. L. Boitnott, E. L. Fasanella, L. E. Jones, and K. H. Lyle, "A History of Full-Scale Aircraft and Rotorcraft Crash Testing and Simulation at NASA Langley Research Center."
[16] A. S. Miguel, "Antimisting fuel kinematics related to aircraft crash landings," *J. Aircr.*, vol. 15, no. 3, pp. 137–142, 1978.
[17] R. G. Thomson and C. Caiafa, "Designing for aircraft structural crashworthiness," *J. Aircr.*, vol. 19, no. 10, pp. 868–874, 1982.
[18] N. A. Moussa, "Flammability of aircraft fuels," SAE Technical Paper, 1990.
[19] M. Wolfson *et al.*, "Characteristics of thunderstorm-generated low altitude wind shear: a survey based on nationwide Terminal Doppler Weather Radar testbed measurements," in *Decision and Control, 1990., Proceedings of the 29th IEEE Conference on*, 1990, pp. 682–688.
[20] M. Piers, "Methods and models for the assessment of third party risk due to aircraft accidents in the vicinity of airports and their implications for societal risk," in *Quantified Societal Risk and Policy Making*, Springer, 1998, pp. 166–204.
[21] J. H. Large, "The implications of 11 September for the nuclear industry," in *Disarmament Forum*, 2003, no. 2.
[22] M. S. Hayden, D. F. Shanahan, L.-H. Chen, and S. P. Baker, "Crash-resistant fuel system effectiveness in civil helicopter crashes," *Aviat. Space. Environ. Med.*, vol. 76, no. 8, pp. 782–785, 2005.
[23] D. W. Mozingo, D. J. Barillo, and J. B. Holcomb, "The Pope Air Force Base aircraft crash and burn disaster," *J. Burn Care Res.*, vol. 26, no. 2, pp. 132–140, 2005.
[24] Accident report, "Steep Climb and Uncontrolled Descent During Takeoff, National Air Cargo, Inc. dba National Airlines, Boeing 747-400 BCF, N949CA, Bagram, Afghanistan, April 29, 2013," 2015.
[25] H. C. Hardee and D. O. Lee, "Expansion of clouds from pressurized liquids," *Accid. Anal. Prev.*, vol. 7, no. 2, pp. 91–102, 1975.
[26] H. C. Hardee, D. O. Lee, and W. B. Benedick, "Thermal hazard from LNG fireballs," *Combust. Sci. Technol.*, vol. 17, no. 5–6, pp. 189–197, 1978.
[27] T. N. O. Y. Book, *Methods for the calculation of the physical effects of the escape of dangerous material*. 1989.
[28] CCPS, *Guidelines for consequence analysis of chemical releases*, vol. 1. Wiley-AIChE, 1999.
[29] W. E. Martinsen and J. D. Marx, "An iproved model for the prediction of radiant heat from fireball," 1999.
[30] J. Moorhouse and M. J. Pritchard, "Thermal radiation hazards from large pool fires and fireballs-a literature review," *IChemE Sym Ser Assess. Major Hazards*, pp. 397–428, 1982.
[31] A. F. Roberts, "Thermal radiation hazards from releases of LPG from pressurised storage," *Fire Saf. J.*, vol. 4, no. 3, pp. 197–212, 1982.
[32] G. M. Makhviladze, J. P. Roberts, and S. E. Yakush, "Fireball during combustion of hydrocarbon fuel releases. I. Structure and lift dynamics," *Combust. Explos. Shock Waves*, vol. 35, no. 3, pp. 219–229, 1999.
[33] G. M. Makhviladze and S. E. Yakush, "Large-scale unconfined fires and explosions," *Proc. Combust. Inst.*, vol. 29, pp. 195–210, 2002.
[34] W. Luther and W. C. Müller, "FDS simulation of the fuel fireball from a hypothetical commercial airliner crash on a generic nuclear power plant," *Nucl. Eng. Des.*, vol. 239, no. 10, pp. 2056–2069, Oct. 2009.
[35] A. Rajendram, F. Khan, and V. Garaniya, "Modelling of fire risks in an offshore facility," *Fire Saf. J.*, vol. 71, pp. 79–85, Jan. 2015.
[36] S. E. Yakush and G. M. Makhviladze, "Large Eddy Simulation of Hydrocarbon Fireballs Institute for Problems in Mechanics," pp. 1–6, 2005.
[37] H. R. Baum and R. G. Rehm, "A simple model of the World Trade Center fireball dynamics," *Proc. Combust. Inst.*, vol. 30, no. 2, pp. 2247–2254, 2005.
[38] V. Shentsov, D. M. C. Cirrone, D. Makarov, and V. Molkov, "simulation of fireball and blast wave from a hydrogen tank rupture in a fire."
[39] A. Shelke, N. K. Maheshwari, B. Gera, and R. K. Singh, "CFD Analysis of Hydrocarbon Fireballs," *Combust. Sci. Technol.*, vol. 189, no. 8, pp. 1440–1466, Aug. 2017.
[40] K. Bhushan, K. Wehrstedt, and H. Krebs, "Boiling Liquid Expanding Vapour Explosion (BLEVE) of peroxy-fuels : Experiments and Computational Fluid Dynamics (CFD) simulation," *Energy Procedia*, vol. 66, no. 1, pp. 149–152,

2015.
[41] K. Wang, Z. Liu, X. Qian, and P. Huang, "Journal of Loss Prevention in the Process Industries Long-term consequence and vulnerability assessment of thermal radiation hazard from LNG explosive fi reball in open space based on full-scale experiment and PHAST," *J. Loss Prev. Process Ind.*, vol. 46, no. 5, pp. 13–22, 2017.
[42] Y. Wang, P. Chatterjee, and J. L. de Ris, "Large eddy simulation of fire plumes," *Proc. Combust. Inst.*, vol. 33, no. 2, pp. 2473–2480, 2011.
[43] T. Poinsot and D. Veynante, "Theoretical and Numerical Combustion (Philadelphia, PA: Edwards)." 2001.
[44] G. H. Yeoh and K. K. Yuen, *Computational fluid dynamics in fire engineering: theory, modelling and practice*. Butterworth-Heinemann, 2009.
[45] K. K. Yuen, *Computational Fluid Dynamics in Fire Engineering*. Butterworth-Heinemann, 2009.
[46] Y. Wang, K. Meredith, P. Chatterjee, N. Krishnamoorthy, X. Zhou, and S. Dorofeev, "Status of FireFOAM development and future plan," in *3rd FM Global Open Source CFD Fire Modeling Workshop, Norwood, MA, USA*, 2011.
[47] I. S. Ertesvåg and B. F. Magnussen, "The eddy dissipation turbulence energy cascade model," *Combust. Sci. Technol.*, vol. 159, no. 1, pp. 213–235, 2000.
[48] C. Jörgen, "Fire Modelling Using CFD," Lund, 1999.
[49] T. F. Smith, Z. F. Shen, and J. N. Friedman, "Evaluation of coefficients for the weighted sum of gray gases model," *J. Heat Transfer*, vol. 104, no. 4, pp. 602–608, 1982.
[50] A. Coppalle and P. Vervisch, "The total emissivities of high-temperature flames," *Combust. Flame*, vol. 49, no. 1, pp. 101–108, 1983.
[51] "NIST-JANAF Thermochemical Tables." [Online]. Available: http://kinetics.nist.gov/janaf/.
[52] G. M. Makhviladze and J. P. Roberts, "Modelling and Scaling of Fireballs from Single-and Two-Phase Hydrocarbon Releases," *Fire Saf. Sci.*, vol. 6, pp. 1125–1136, 2000.